RSC Advances

PAPER

View Article Online
View Journal | View Issue

Cite this: *RSC Adv.*, 2016, **6**, 75707

Preparation of CoNC catalysts *via* heating a mixture of cobaltporphyrin and casein for ethylbenzene oxidation

Congqiang Yang,[a] Yuan Chen,[a] Sufang Zhao,[a] Runliang Zhu[b] and Zhigang Liu*[a]

Received 4th July 2016
Accepted 29th July 2016

DOI: 10.1039/c6ra17114a

www.rsc.org/advances

Biomass-derived cobalt-coordinated N-doped carbon (CoNC) for C–H bond oxidation is synthesized by a facile procedure based on pyrolysis of cobaltporphyrin with natural, amino acid-rich biomass casein as a supplementary nitrogen source. The catalysts are characterized by techniques such as transmission electron microscopy (TEM), X-ray diffraction (XRD), Raman spectroscopy and X-ray photoelectron spectroscopy (XPS). The obtained CoNC catalyst has a high metal content and dispersion and shows superior catalytic performance in C–H bond oxidation with molecular oxygen as oxidant under solvent-free conditions. This is attributed to the promotion of the Co–N$_x$ moiety originating from cobaltporphyrin. Moreover, the catalyst shows remarkable stability and can be recycled several times without losing its activity.

1. Introduction

Oxidation of carbon–hydrogen (C–H) bonds to oxygenated derivatives is of great importance in the chemical, pharmaceutical and petrochemical industries as they are widely used for the production of intermediates.[1–5] Industrially performed catalytic oxidation processes, such as oxidation of ethylbenzene, often suffer from drawbacks such as high cost, negative environmental impact and a large amount of corrosive waste.[6,7] With a view to a green catalytic oxidation process, molecular oxygen as an eco-friendly, effective and economical oxidant is preferred.[2,8–10] However, catalytic oxidation of carbon–hydrogen bonds in an oxygen-based system remains a challenging topic in contemporary chemical research as the C–H bond is inert.[4,11]

In recent years, nitrogen-doped carbon materials have attracted a lot of interest owing to its unique properties such as high thermal conductivity, excellent electric conductivity and high binding ability.[12,13] Carbon nitrides are promising candidates to complement carbon in diverse materials applications.[14,23] It has been reported that nitrogen-doped carbon makes catalytic oxidation of ethylbenzene in an oxygen-based system possible.[15–17] However, its catalytic performance needs to be further improved. Ning *et al.*[18] have confirmed that the rational selection of N source has a large effect on the activity of the catalysts, and the nature of nitrogen functionalities is greatly affected by the structure of nitrogen precursors. Recently, the research focus has shifted from N-containing hazardous inorganic or organic chemicals to renewable and bountiful biomass resources as precursors in the preparation of functional carbon materials with high nitrogen content.[19,20] Several N-rich natural resources, including egg-white protein,[21] ginkgo leaves,[22] chitosan,[23] silk fibroin,[24] soybean[25] have been reported to prepare N-doped carbon materials and used as effective catalysts.

Casein, main composition of the milk, is rich in amino acids such as glutamic, proline, leucine, lysine, valine and tyrosine, which makes it an attractive N source. It as well possesses advantages of cheaply and readily available, environmental friendly. In addition, catalytic materials have been concentrated on composite structure with metallic actives as their performance can be significantly improved by the use of a co-catalyst.[26,27] As widely studied biomimetic catalysts, cobaltporphyrins have been found to be excellent catalysts for aziridination, C–H amination, and cyclopropanation.[28–30] Its unique characteristics similar to models of cytochrome P450 might be exploited in preparation of efficient metal-doped carbon nitrides materials for a wider range of applications.

In this study, a simple approach for the synthesis of CoNC catalyst with cobaltporphyrin (serves as metal and N source) and casein (serves as supplementary nitrogen source) is described. Catalytic performance of this material in the heterogeneous oxidation of ethylbenzene is demonstrated. The CoNC catalysts are characterized by techniques such as TEM, XRD, Raman and XPS.

2. Experimental

2.1 Characterizations

The morphologies of samples are examined by TEM and high-resolution transmission electron microscopy (HRTEM) on an

---

[a] *State Key Laboratory of Chemo/Biosensing and Chemometrics, College of Chemistry and Chemical Engineering, Hunan University, Changsha 410082, Hunan, China. E-mail: liuzhigang@hnu.edu.cn; Tel: +86-731-8882-3327*

[b] *Guangdong Provincial Key Laboratory of Mineral Physics and Material Research & Development, Guangzhou Institute of Geochemistry, Chinese Academy of Sciences, Guangzhou 510640, China*

FEI Tecnai G2 Spirit electron microscope at an accelerating voltage of 120 kV. XPS is conducted using a VG ESCA 2000 with an $Mg_{K\alpha}$ as the source and using the C 1s peak at 284.6 eV as an internal standard. Raman spectra are collected on a Bruker RFS 100/S spectrometer with 514 nm laser excitation. XRD patterns are acquired on a D8-Advanced diffractometer system from Bruker with $Cu_{K\alpha}$ radiation ($\lambda = 1.5418$ Å). Co content in catalyst is analyzed by Atomic Absorption Spectrometry (AAS) on VARIAN (AA240).

2.2 Synthesis of cobaltporphyrin

The compound is synthesized by referring to the following procedures. 5.56 g benzaldehyde is added into 200 ml propanoic acid and heated to reflux, then 4.03 g freshly distilled pyrrole is added into the system dropwise. The obtained product is cooled overnight, collected by filtration and washed with cold water. The precipitate is purified by column chromatography. Then, the product tetraphenylporphyrin is obtained. 1.0 g as-synthesized sample is added to 100 ml *N*,*N*-dimethylformamide (DMF). When mixture is heated to reflux, 2.0 g metal chloride is gradually added into the system. The solution is allowed to cool overnight. The obtained product is filtered and washed repeatedly with cold water, and the product is achieved.

2.3 Preparation of CoNC-*x* composites

The synthesis of CoNC-*x* samples has been carried out by loading different amount of cobaltporphyrin ($x = 0.1$, 0.2, 0.3, 0.5, 0.8 g, where x is the exact weight of cobaltporphyrin used per 0.5 g casein) onto the casein and then calcinated under nitrogen atmosphere. In a typical procedure, cobaltporphyrin is dissolved in 20 ml CH_2Cl_2 and stirred for 10 min. Then 0.5 g casein is added into the solution, and the mixture is heated to reflux at 40 °C for 24 h. The CH_2Cl_2 is completely removed using a rotary evaporator. The obtained solid sample dried at 60 °C for 4 hours is transferred into a quartz boat and annealed in 100 $cm^3\ min^{-1}$ of flowing N_2 at 500 °C for 1 h. The sample is then allowed to cool in the tube furnace to room temperature. For comparison, cobaltporphyrin and casein are pyrolyzed using similar method and the obtained products are designed as CoNC-PR and NC, respectively.

2.4 Preparation of Co/NC-0.5

The catalyst with Co nanoparticles supported on NC material is synthesized by following procedures. $CoCl_2\cdot 6H_2O$ (0.18 g) is dissolved in 20 ml CH_2Cl_2. Then as-prepared NC material (0.2 g) is added into the solution, and the mixture is heated to reflux at 40 °C for 24 h. The CH_2Cl_2 is completely removed using a rotary evaporator. The obtained solid sample is transferred into a quartz boat and annealed in 100 $cm^3\ min^{-1}$ of flowing N_2 at 500 °C for 1 h. The product is designed as Co/NC-0.5 (the molar content of metal ions is equal to that of CoNC-0.5).

2.5 Catalytic tests

The oxidation of ethylbenzene over CoNC-*x* using O_2 as the oxidant is carried out in a 50 ml teflon-lined stainless steel batch reactor. Typically, 10.0 ml of ethylbenzene and 30 mg of catalyst are placed in the reactor. After being sealed, the reactor is heated to the reaction temperature (120 °C), with continuous magnetic stirring. Upon heating to the desired temperature the O_2 pressure is increased to 0.8 MPa and O_2 is fed continuously to maintain constant pressure. The reaction is carried out at 120 °C for 5 h. After reaction, the samples are analyzed by GC (ShimadzuGC-2014) equipped with a capillary column (RTX-5, 30 m, φ 0.25 mm) and FID detector with 1 $ml\ min^{-1}$ nitrogen as carrier gas. The programmed temperature was conduced from 60 °C to 120 °C and then kept at 120 °C for 3 min. The product is quantified by internal standard method using bromobenzene and 1,4-dichlorobenzene as reference.

3. Results and discussion

3.1 Characterizations

As illustrated in Fig. 1, samples obtained are denoted as CoNC-*x* (where *x* is the exact quality of cobaltporphyrin used per 0.5 g

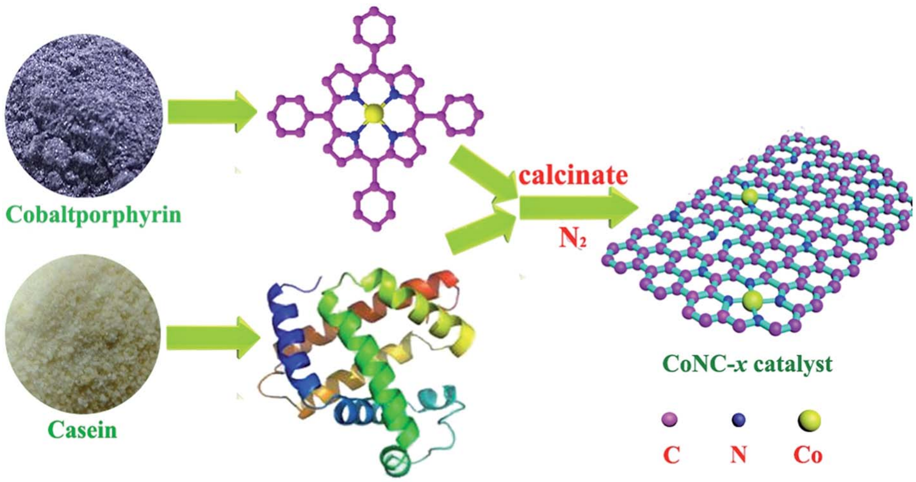

Fig. 1 Schematic illustration of the synthesis of CoNC-*x* from cobaltporphyrin and casein under N_2 protection.

casein). For comparison, cobaltporphyrin and casein are pyrolyzed using similar method and the obtained products are designed as CoNC-PR and NC, respectively. The morphology and structural features of the as-prepared samples are examined by TEM and high-resolution TEM (HRTEM). The spongy N-doped carbon layer deriving from casein with hollow carbon nanocages can be clearly observed in Fig. 2a. As shown in Fig. 2b and e, the Co nanoparticles (NPs) of CoNC-*x* are uniformly embedded in the carbon matrix with the dark spots depicting metal crystallite formation. The Co NPs are rarely aggregated, indicating a good dispersion in the carbon structure. The size distribution histograms (Fig. 2d–f) demonstrate the average size of cobalt NPs is about 3.6, 3.8 and 6.3 nm for CoNC-0.2, CoNC-0.5 and CoNC-PR, respectively. Co particle size in CoNC-*x* is smaller than that of CoNC-PR. This implies that casein can effectively prevent Co NPs from agglomerating. This can be attributed to the introduction of extra nitrogen atoms increasing the number of anchoring sites, improving the dispersion of metal ions.[31] HRTEM images clearly reveal that the as-synthesized CoNC-*x* possess a crystalline structure with a lattice spacing of 0.21 nm, which is in good agreement with the (111) lattice spacing of metallic Co, and also uncovers the lattice fringes of Co_3O_4 (220) planes with a spacing of 0.29 nm.[32,33]

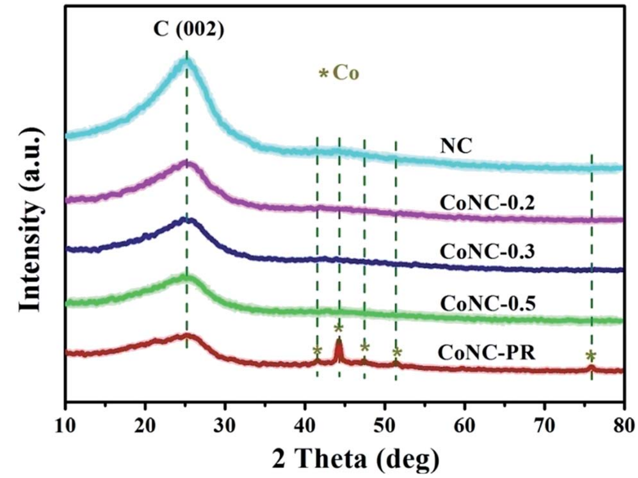

Fig. 3 XRD patterns of NC, CoNC-*x* ($x = 0.2, 0.3, 0.5$), and CoNC-PR.

The X-ray diffraction (XRD) patterns of samples in Fig. 3 show a broad characteristic peaks located at about 27.4° which can be indexed to the (002) planes of graphite.[4,33,34] The XRD pattern of CoNC-PR exhibits XRD peaks at around 44.3°, 51.6° and 75.8° implying the presence of metallic cobalt in the

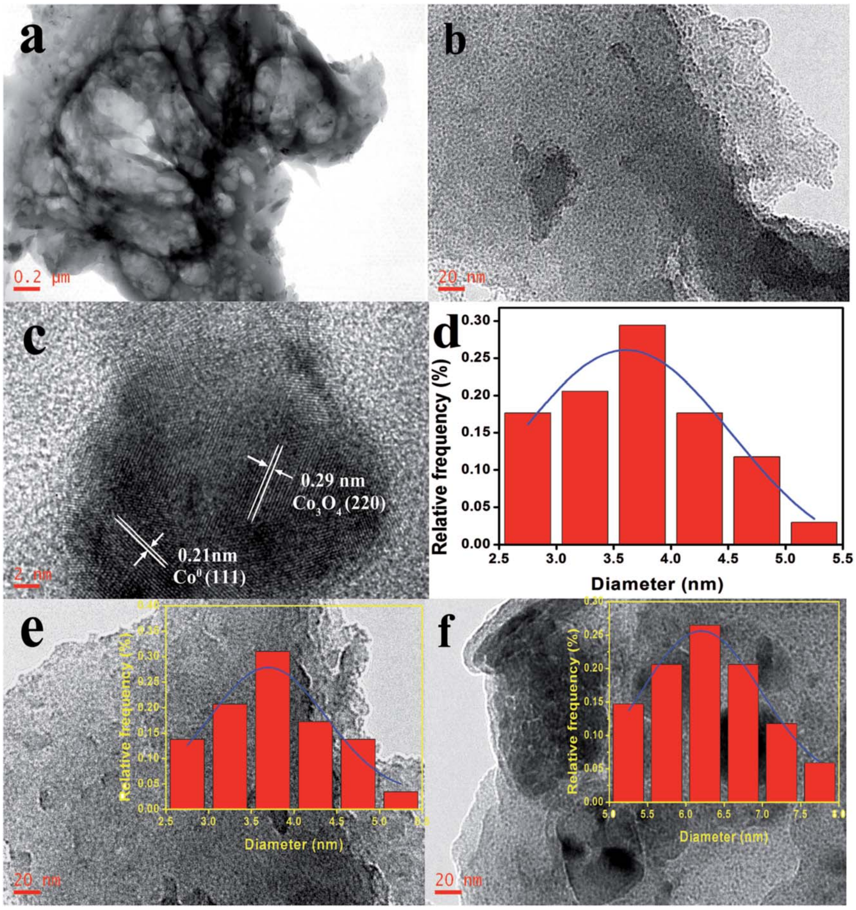

Fig. 2 TEM images of (a) NC, (b) CoNC-0.5, (c) HRTEM images of CoNC-0.5, (d) particle size distribution histogram of CoNC-0.5, (e) TEM images of CoNC-0.2, (f) TEM images of CoNC-PR, inset (e), (f) are corresponding particle size distribution histogram.

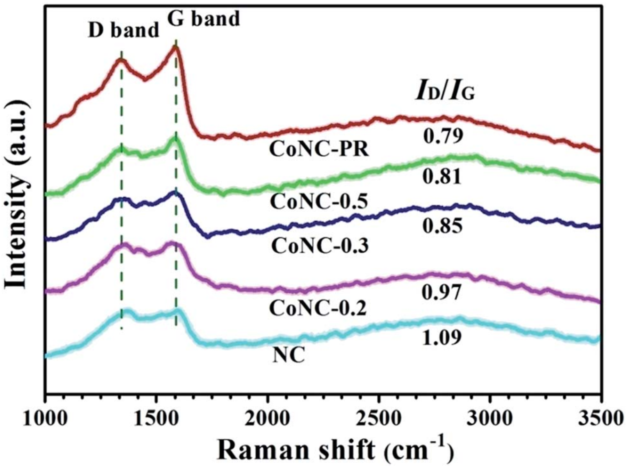

Fig. 4 Raman spectra of NC, CoNC-*x* ($x = 0.2$, 0.3, 0.5), and CoNC-PR.

CoNC-PR hybrid composite.[35,36] Peaks of metallic cobalt have not been detected in XRD patterns of CoNC-*x* probably due to the smaller size and higher dispersion of Co NPs in nitrogen-doped carbon.[37] These characters are attributed to casein which restrains the growth of Co NPs and improves metal dispersion through increasing anchoring sites.

To further investigate the degree of graphitization and doping status of CoNC-*x*, CoNC-PR and NC, Raman spectroscopy is used. As shown in Fig. 4, all these materials have an obvious D band at 1338 cm^{-1} which is associated with defects including bonding disorders and vacancies in the graphite lattice, and a G band at 1578 cm^{-1} which is corresponding to graphitic carbon.[38–41] The intensity ratio of D band *versus* G band (I_D/I_G) is a significant parameter to reflect the defect and disorder level in the graphitic carbon layers.[42,43] The I_D/I_G value of NC (1.09) is higher than those of CoNC-0.2 (0.97), CoNC-0.3 (0.85), CoNC-0.5 (0.81) and CoNC-PR (0.79). The ratio of I_D/I_G increases accompanied by a increase in the relative content of casein indicating that casein can improve defect level of the catalyst. The higher ratio of CoNC-*x* than that of CoNC-PR demonstrates excellent structure of CoNC-*x* derived from biomass casein.

The X-ray photoelectron spectroscopy (XPS) analysis is used to investigate surface compositions and surface chemical states of the catalysts. As shown in Fig. 5a, a set of peaks corresponding to C 1s (284.6 eV), N 1s (401.0 eV), O 1s (531.6 eV) and Co 2p (780.0 eV) is observed. The spectral deconvolution of the C 1s high-resolution XPS spectrum (Fig. 5b) reveals the chemical environment of carbon. The C 1s spectrum shows three peaks at 283.6, 284.8, 285.4 eV, which are assigned to C=C, C=N, and C–N, respectively.[38,44] The high-resolution XPS spectrum (Fig. 5c) of the N 1s peaks at 397.5, 398.8, and 400.2 eV, is

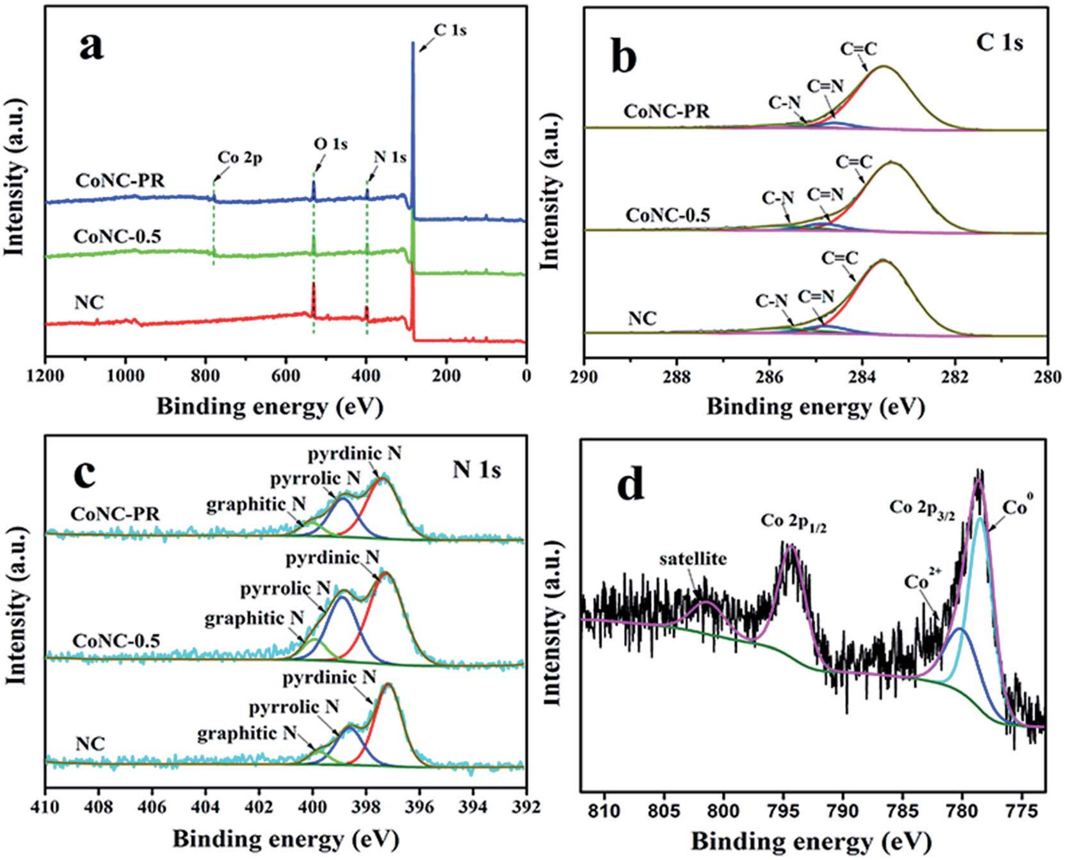

Fig. 5 (a) XPS survey of samples, high-resolution XPS spectra of (b) C 1s, (c) N 1s and (d) Co 2p regions of CoNC-*x*.

corresponding to the pyridinic C=N π* state, amino-type and graphitic-type N, respectively..[44,45] It has been reported that amino-type N inherits functional groups such as catechol and N–H groups could effectively coordinate with Co in formation of Co–N_x species.[35] In cobalt region (Fig. 5d), the first peak at around 778.2 eV is consistent with the Co $2p_{3/2}$ binding energy of Co in a zero-valent state.[36] Generally speaking, thermal treatment of metalloporphyrin can generate groups containing nitrogen that serve as coordination centers for metal ions where metal–N_x is formed. The binding energy of 781.5 eV of the Co $2p_{3/2}$ is generally ascribed to Co–N_x.[46] Peak characteristic for oxidic Co with the typical binding energy of 795.3 eV of the Co $2p_{1/2}$ is found.[47] Furthermore, a shake-up satellite peak at 802.9 eV suggests that the oxidic Co is mainly composed of Co_3O_4.[48] Surface species composition is depicted in Table 1. The metal content of CoNC-PR is up to 1.70 at% indicating that cobaltporphyrin is an excellent metal precursor. The higher N content of NC (8.47 at%) compared to that of CoNC-PR (5.05 at%) suggests that casein can act as a novel and efficient N source. CoNC-*x* possesses higher N content than that of CoNC-PR demonstrates the advantageous role of casein in improving nitrogen content of catalysts. Meanwhile, the relative content of Co ions increases, total nitrogen content slightly decreases with an increase in the amount of cobaltporphyrin. The results above suggest that the N and Co NPs dosage can be facilely tuned by changing the mass ratio of casein and cobaltporphyrin.

3.2 Activity measurement

Catalytic testing is performed for oxidation of ethylbenzene over CoNC-*x*, CoNC-PR and NC. The corresponding catalytic performances are summarized in Table 2. The blank run (entry 1, Table 2) gives conversion of 7%. However, NC exhibits remarkably improved catalytic activity with the conversion of 15% (entry 2, Table 2). This observation suggests that NC material can help to promote the activation of C–H bond.

Table 1 The ratio analysis of the surface species of the catalysts

				N (at%)			
Samples	C (at%)	O (at%)	Co (at%)	Total	PD[a] (%)	PR (%)	GH (%)
NC	81.30	10.22	—	8.47	43.69	49.66	3.95
CoNC-PR	86.26	6.99	1.70	5.05	62.40	30.25	7.35
CoNC-0.2	81.27	9.76	0.90	7.63	58.02	34.69	7.29
CoNC-0.3	85.84	7.91	1.20	5.84	58.00	34.71	7.29
CoNC-0.5	83.94	8.59	1.22	5.45	62.60	30.15	7.25

[a] PD = pyridinic N, PR = pyrrolic N, GH = graphitic N.

Table 2 Catalytic performances of ethylbenzene oxidation over NC, CoNC-*x* and CoNC-PR[a]

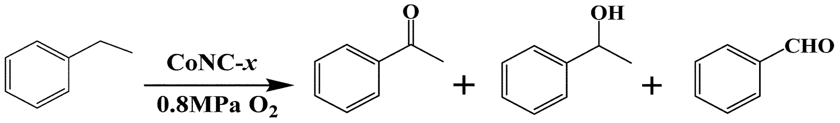

			Sel.[b] (%)		
Entry	Catalyst	Conv. (%)	AP	PA	BD
1	Blank	7	77	20	3
2	NC	15	76	18	6
3	CoNC-PR	17	73	21	6
4	CoNC-0.1	18	74	18	8
5	CoNC-0.2	19	75	19	6
6	CoNC-0.3	20	75	19	6
7	CoNC-0.5	24	75	20	5
8	CoNC-0.8	19	76	21	3
9[c,d]	CoNC-0.5	9	73	22	5
10[e]	CoNC-0.5	20	75	20	5
11	Co/NC-0.5	17	78	20	2

[a] Typical conditions: 10 ml of ethylbenzene, 30 mg of catalyst, O_2 (0.8 MPa), 120 °C, 5 h. [b] Corresponding selectivities (%) to acetophenone (AP), phenethyl alcohol (PA), benzaldehyde (BD). [c] Catalyst was immersed in l mol L^{-1} KSCN solution at 80 °C for 5 hours. [d] 0.1 g of KSCN powder should be added into the reaction system. [e] A thermal treatment was applied to catalyst cycling 6 times at 300 °C for an hour.

CoNC-0.5 gives conversion of 24% which is higher than that of blank and NC. This may be attributed to the promotion of Co–N$_x$ particles.[49,50] The role of Co–N$_x$ moiety can be confirmed by using small molecules to form highly stable metal–ligand coordination intermediate compounds to interrupt the reaction.[51–54] When Co–N$_x$ species are poisoned, significant loss of catalytic activity is observed (entry 9, Table 2). To further verify the role of Co–N$_x$, a control-experiment is carried out. As a comparison, Co/NC-0.5 with Co NPs supported on NC material gives conversion up to 17% (entry 11, Table 2) which is much lower than that of CoNC-0.5 (entry 7, Table 2). This may be attributed to that Co ions doped in N–C structure can promote the generation of free radicals by interaction of the metal clusters with oxygen.[55,56] The higher catalytic performance of CoNC-0.5 shows that Co–N$_x$ moieties which act as a co-catalyst can effectively improve the catalytic activity of NC catalyst.

Interestingly, although the relative content of Co NPs decreases, CoNC-*x* gives higher conversion (entry 4–8, Table 2) than CoNC-PR. According to the analysis above, this can be attributed to (i) casein enhances defect and disorder level in the catalyst, which usually dominate their properties and also the catalytic activity; (ii) casein improves dispersion of Co NPs through increasing the number of anchoring sites in the carbon structure; (iii) casein can increase the nitrogen content in material and enhance its catalytic activity by tailoring its electron-donor properties.

According to the results above, both casein and Co NPs can enhance the catalytic performance. In CoNC-*x* catalysts, conversion of ethylbenzene increases accompanied by a increase in relative content of cobaltporphyrin may be attributed to increasing content of Co–N$_x$ (entry 4–7, Table 2). However, the catalytic performance decreases when content of cobaltporphyrin further increases (entry 8, Table 2). This may be attributed to the aggregation of excess metal ions, and thus lead to a decline in activity. Since CoNC-0.5 was found to be the best catalyst for the oxidation of ethylbenzene, it was also used in further experiments and showed excellent catalytic performance, the results of which are summarized in Table 3.

Table 3 Molecular oxygen oxidation of substituted hydrocarbons to ketone using CoNC-0.5[a]

Entry	Substrate	Main product	*T* (°C)	Conv. (%)	Sel. (%)
1	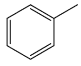	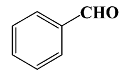	160	14	67
2	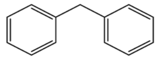	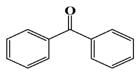	100	30	69
3	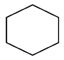	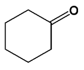	160	5	63
4	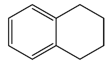	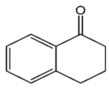	100	61	84
5	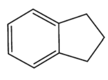	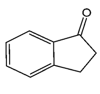	100	77	92
6	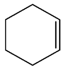	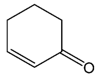	100	67	56
7[b]	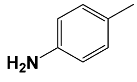	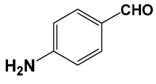	120	32	86

[a] Typical conditions: 10 ml of substrate, 30 mg of catalyst, O_2 (0.8 MPa), 5 h. [b] 3 g of substrate, 10 mg of catalyst, O_2 (0.8 MPa), 5 h.

4. Reusability of the catalyst

For metal catalysts, stability is a strongly important factor as metal ions are easily oxidized during oxidation reaction which will result in the decrease of catalytic activity. However, the as-prepared catalyst in this paper exhibits outstanding stability which can be reused for several cycles without loss of activity. As shown in Fig. 6, there remains 91% activity after recycling 6 times. A thermal treatment on reused catalyst is applied to burn the covered intermediates on the active sites and edges of the catalyst (entry 11, Table 2).[39] It gives conversion of 20%, a little lower than that of 21% at sixth run. The mild decrease in catalytic activity may be attributed to the loss of catalyst in the process of transfer. The result shows that there almost no intermediate covers on the surface of catalyst. The structure and composition of the used catalyst is investigated by XPS. As shown in Fig. 7, no apparent structural changes are found in XPS spectra of CoNC-0.5 before and after reaction. The Co content in fresh and reused CoNC-0.5 catalysts was determined by AAS (Table 4). About 6.2% metal particles detached from the catalyst and migrated to the liquid phase. The slight loss of metal particles may be attributed to the powerful interaction between metal particles and N–C moiety, which stabilize Co species in the electron-rich N-doped carbon structure mainly through Co–N bonds and effectively prevent metal particles from detaching

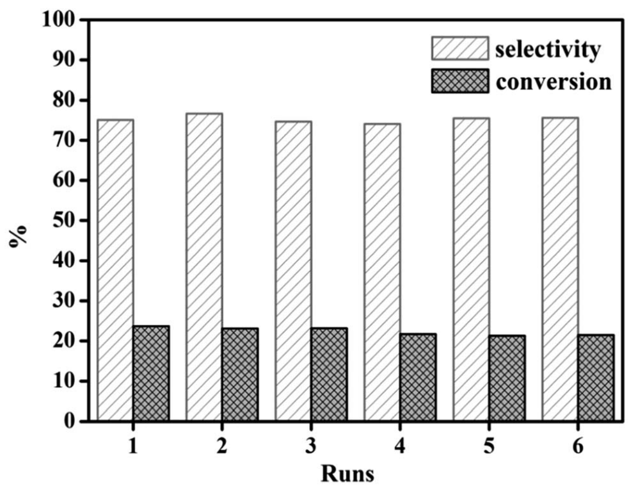

Fig. 6 Recyclability of CoNC-0.5 in ethylbenzene oxidation. Reactions are carried out at 120 °C for 5 h with 10 ml ethylbenzene and 30 mg CoNC-0.5 under 0.8 MPa oxygen pressure.

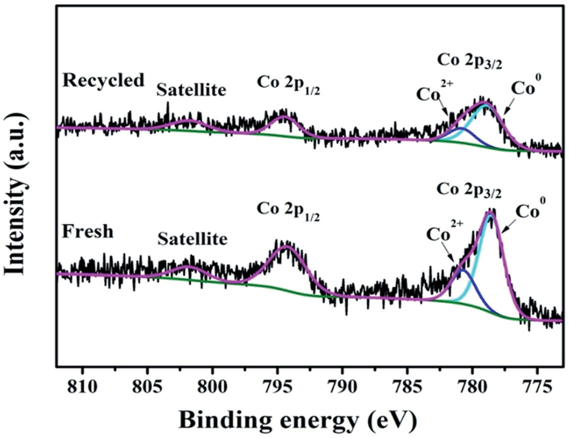

Fig. 7 High-resolution XPS spectra of Co 2p regions of fresh and recycled CoNC-0.5.

Table 4 Co content determined by analysis of atomic absorption spectrometry (AAS)

	Co content (mg)	
Catalyst[a,b]	Fresh	Reused[c]
CoNC-0.5	1.13	1.06

[a] 30 mg catalyst. [b] Catalyst was immersed in l mol L^{-1} HNO_3 solution at 60 °C for 24 h to detach metal particles. [c] The catalyst has been recycled for three times.

and aggregation. To sum up, those three aspects above are responsible for superior reusability of the sample.

5. Conclusions

In this work, cobalt-coordinated N-doped carbon is prepared by pyrolyzing cobaltporphyrin under N_2 atmosphere with casein as supplementary nitrogen source. The CoNC catalyst originated from cobaltporphyrin has high metal content, dispersion and small particle size. The catalyst shows promising catalytic activity for C–H bond oxidation with Co–N_x plays the role of active site. Moreover, it is highly stable and can be recycled several times without losing its activity. Thus, this study has demonstrated that pyrolysis of cobaltporphyrin with casein as supplementary nitrogen source might be a viable route to design efficient and durable CoNC catalysts with small particle size, high metal content for C–H bond activation.

Acknowledgements

The authors gratefully acknowledge the financial support from National Natural Science Foundation of China (No. 21103045, 1210040, 1103312), the Fundamental Research Funds for the Central Universities, the State Key Laboratory of Heavy Oil in China (No. SKCHOP201504) and the Key Laboratory of Mineralogy and Metallogeny in Chinese Academy of Sciences (No. KLMM20150103).

References

1 M. S. Chen and M. C. White, *Science*, 2010, **327**, 566.
2 X. H. Li, X. C. Wang and M. Antonietti, *ACS Catal.*, 2012, **2**, 2082.
3 Z. Y. Li, L. R. Hu, Q. Y. Liu, C. G. Ning, H. Chen, S. G. He and J. N. Yao, *Chem.–Eur. J.*, 2015, **21**, 17748.
4 Y. Wang, H. R. Li, J. Yao, X. C. Wang and M. Antonietti, *Chem. Sci.*, 2011, **2**, 446.
5 M. Arshadi, M. Ghiaci, A. A. Ensafi, H. Karimi-Maleh and S. L. Suib, *J. Mol. Catal. A: Chem.*, 2011, **338**, 71.
6 D. R. Dreyer, H.-P. Jia and C. W. Bielawski, *Angew. Chem., Int. Ed.*, 2010, **49**, 6686.
7 Q. Yang, W. Y. Wang, Y. X. Zhao, J. J. Zhu and L. H. Wang, *RSC Adv.*, 2015, **5**, 54978.
8 D. X. Yang, T. Jiang, T. B. Wu, P. Zhang, H. L. Han and B. X. Han, *Catal. Sci. Technol.*, 2016, **6**, 193.
9 J. Fan, Y. H. Dai, Y. L. Li, N. F. Zhang, J. F. Guo, X. Q. Yan and G. D. Stucky, *J. Am. Chem. Soc.*, 2009, **131**, 15568.
10 L. L. Geng, M. Zhang, W. X. Zhang, M. J. Jia, W. F. Yan and G. Liu, *Catal. Sci. Technol.*, 2015, **5**, 3097.
11 C. Chen, S. Shi, M. Wang, H. Ma, L. P. Zhou and J. Xu, *J. Mater. Chem. A*, 2014, **2**, 8126.
12 C. L. Zhang, L. H. Kang, M. Y. Zhu and B. Dai, *RSC Adv.*, 2015, **5**, 7461–7468.
13 N. Fechler, G. A. Tiruye, R. Marcilla and M. Antonietti, *RSC Adv.*, 2014, **4**, 26981–26989.
14 X. L. Yuan, M. Zhang, X. D. Chen, N. H. An, G. Liu, Y. Liu, W. X. Zhang, W. F. Yan and M. J. Jia, *Appl. Catal., A*, 2012, **439**, 149.
15 Y. J. Gao, G. Hu, J. Zhong, Z. J. Shi, Y. S. Zhu, D. S. Su, J. G. Wang, X. H. Bao and D. Ma, *Angew. Chem., Int. Ed.*, 2013, **52**, 2109.
16 A. B. Chen, Y. F. Yu, R. J. Wang, Y. H. Yu, W. W. Zang, P. Tang and D. Ma, *Nanoscale*, 2015, **7**, 14684.
17 H. Yu, F. Peng, J. Tan, X. W. Hu, H. J. Wang, J. Yang and W. X. Zheng, *Angew. Chem.*, 2011, **123**, 4064.
18 X. M. Ning, H. Yu, F. Peng and H. J. Wang, *J. Catal.*, 2015, **325**, 136.
19 X. Liu, Y. Zhou, W. Zhou, L. Li, S. Huang and S. Chen, *Nanoscale*, 2015, **7**, 6136.
20 C. Lavorato, A. Primo, R. Molinari and H. Garcia, *Chem.–Eur. J.*, 2014, **20**, 187.
21 K. L. Wang, H. Wang, S. Ji, H. Feng, V. Linkov and R. F. Wang, *RSC Adv.*, 2013, **3**, 12039.
22 F. Pan, Z. Cao, Q. Zhao, H. Liang and J. Zhang, *J. Power Sources*, 2014, **272**, 8.
23 A. Primo, E. Sánchez, J. M. Delgado and H. García, *Carbon*, 2014, **68**, 777.
24 C. Z. Guo, W. Liao and C. G. Chen, *J. Power Sources*, 2014, **269**, 841.
25 H. Yang, H. Li, H. Wang, S. Ji, J. Key and R. Wang, *J. Electrochem. Soc.*, 2014, **161**, 795.

26 F. Fina, H. Ménard and J. T. S. Irvine, *Phys. Chem. Chem. Phys.*, 2015, **18**, 4635.
27 J. F. Xie and Y. Xie, *Chem.–Eur. J.*, 2015, **21**, 1.
28 G. Y. Gao, J. D. Harden and X. P. Zhang, *Org. Lett.*, 2005, **7**, 3191.
29 A. Caselli, E. Gallo, F. Ragaini, F. Ricatto, G. Abbiati and S. Cenini, *Inorg. Chim. Acta*, 2006, **359**, 2924.
30 J. V. Ruppel, J. E. Jones, C. A. Huff, R. M. Kamble, Y. Chen and X. P. Zhang, *Org. Lett.*, 2008, **10**, 1995.
31 R. F. Nie, H. Z. Jiang, X. H. Lu, D. Z. Zhou and Q. H. Xia, *Catal. Sci. Technol.*, 2016, **6**, 1913.
32 H. Y. Jin, J. Wang, D. F. Su, Z. Z. Wei, Z. F. Pang and Y. Wang, *J. Am. Chem. Soc.*, 2015, **137**, 2688.
33 M. Q. Wang, W. H. Yang, H. H. Wang, C. Chen, Z. Y. Zhou and S. G. Sun, *ACS Catal.*, 2014, **4**, 3928.
34 J. Xu, K. Shen, B. Xue and Y. X. Li, *J. Mol. Catal. A: Chem.*, 2013, **372**, 105.
35 Y. H. Su, Y. H. Zhu, H. L. Jiang, J. H. Shen, X. L. Yang, W. J. Zou, J. D. Chen and C. Z. Li, *Nanoscale*, 2014, **6**, 15080.
36 L. L. Fu, Y. Chen and Z. G. Liu, *J. Mol. Catal. A: Chem.*, 2015, **408**, 91.
37 B. Qiu, C. Pan, W. Qian, Y. Peng, L. Qiu and F. Yan, *J. Mater. Chem. A*, 2013, **1**, 6373.
38 Z. G. Wang, P. J. Li, Y. F. Chen, J. B. Liu, H. J. Tian, J. H. Zhou, W. L. Zhang and Y. R. Li, *J. Mater. Chem. C*, 2014, **2**, 7396.
39 Y. Chen, L. L. Fu and Z. G. Liu, *Chem. Commun.*, 2015, **51**, 16637.
40 M. M. Fan, C. L. Zhu, Z. Q. Feng, J. Z. Yang, L. Liu and D. F. Sun, *Nanoscale*, 2014, **6**, 4882.
41 C. Z. Guo, W. L. Liao, Z. B. Li, L. T. Sun and C. G. Chen, *Nanoscale*, 2015, **7**, 15990.
42 X. G. Duan, Z. M. Ao, H. Q. Sun, S. Indrawirwan, Y. X. Wang, J. Kang, F. L. Liang, Z. H. Zhu and S. B. Wang, *ACS Appl. Mater. Interfaces*, 2015, **7**, 4169.
43 C. H. Choi, S. H. Park and S. I. Woo, *ACS Nano*, 2012, **6**, 7084.
44 J. Y. Liu, H. Y. Chang, Q. D. Truong and Y. C. Ling, *J. Mater. Chem. C*, 2013, **1**, 1713.
45 P. P. Su, H. Xiao, J. Zhao, Y. Yao, Z. G. Shao, C. Li and Q. H. Yang, *Chem. Sci.*, 2013, **4**, 2941.
46 S. Pylypenko, S. Mukherjee, T. S. Olson and P. Atanassov, *Electrochim. Acta*, 2008, **53**, 7875.
47 R. V. Jagadeesh, H. Junge, M. M. Pohl, J. Radnik, A. Brückner and M. Beller, *J. Am. Chem. Soc.*, 2013, **135**, 10776.
48 D. K. Huang, Y. P. Luo, S. H. Li, B. Y. Zhang, Y. Shen and M. K. Wang, *Nano Res.*, 2014, **7**, 1054.
49 W. G. Liu, L. L. Zhang, W. S. Yan, X. Y. Liu, X. F. Yang, S. Miao, W. T. Wang, A. Q. Wamg and T. Zhang, *Chem. Sci.*, DOI: 10.1039/c6sc02105k.
50 S. S. Shang, L. Y. Yang, W. Dai, B. Chen, Y. Lv and S. Gao, *Catal. Sci. Technol.*, 2016, **6**, 5746.
51 D. Singh, K. Mamtani, C. R. Bruening, J. T. Miller and U. S. Ozkan, *ACS Catal.*, 2014, **4**, 3454.
52 D. von Deak, D. Singh, E. J. Biddinger, J. C. King, B. Bayram, J. T. Miller and U. S. Ozkan, *J. Catal.*, 2012, **285**, 145.
53 C. Q. Yang, L. L. Fu, R. L. Zhu and Z. G. Liu, *Phys. Chem. Chem. Phys.*, 2016, **18**, 4635.
54 T. Y. Chen, H. Yu, F. Peng, H. J. Wang, B. S. Zhang and D. S. Su, *Catal. Sci. Technol.*, 2016, **6**, 1007.
55 A. Santiago-Portillo, S. Naralon, F. G. Cirujano, F. X. Llabrés i Xamena, M. Alvaro and H. Garcia, *ACS Catal.*, 2015, **5**, 3216.
56 L. L. Zhang, A. Q. Wang, W. T. Wang, Y. Q. Huang, X. Y. Liu, S. Miao, J. Y. Liu and T. Zhang, *ACS Catal.*, 2015, **5**, 6563.